Journal of Nepal Hydrogeological Association (JNHA), Vol (2), 91-111 (2025)
ISSN: 3059-9725 (Online)
https://doi.org/10.3126/jnha.v2i1.85384

RESEARCH ARTICLE

Evaluating the Topographical Factors Contributing to Landslide Occurrences in the Thuligad Watershed of Far-Western Province, Nepal

***Bharat Prasad Bhandari[1,2] , Tekendra Bahadur Saud[2], Prakash Bahadur Ayer[2]**

[1]Central Department of Environmental Science, Tribhuvan University, Nepal
[2]College of Applied Sciences, Tribhuvan University, Kathmandu, Nepal
**Corresponding author: bbhandri@cdes.edu.np*

***(Submission Date**: 2 July, 2025; **Accepted Date:** 16 August, 2025)*

ABSTRACT

The Thuligad watershed in the Farwestern Province has been facing a substantial landslide challenge for a long time, especially during the monsoon season. The harsh topography, characterized by numerous steep slopes, is prevalent across the Thuligad watershed, resulting in a significant incidence of landslides across the area.This research aims to evaluate the impact of topographical factors to trigger landslide within the Thuligad watershed located in the Sudurpaschim province of Nepal. The work began with the use of satellite imagery and ArcGIS to develop a comprehensive spatial and temporal inventory map of landslides. The map illustrating the five topographical factors was generated utilizing a 12.5 m digital elevation model obtained from Alaska Satellite Fascility of United States Geological Survey. The dimensions of the pixel sizes pertaining to the subclasses of factors, as well as those associated with landslides within these subclasses, were ascertained. In a comparable manner, the quantity of landslides identified in relation to aspect, curvature, and slope was derived from both field observations and spatial analyst tool of ArcGIS. The dimensions of the landslide were determined through area measurement and subsequently correlated with the classification of the slope. A statistical index model was employed to ascertain the significant relationship between topographical factors and landslides. A notable positive correlation exists between slope and landslide density; however, the incidence and extent of landslides are greater within the slope range of 30 to 45 degrees. The density of landslides is markedly higher on slopes exceeding 60 degrees. The concave slope with a southern aspect exhibits a notably high incidence of landslides. The topographical wetness index exhibits an inverse correlation with landslide occurrences. The stream power index exhibits a positive correlation with the frequency of landslides. The interplay of slope, stream power index, aspect, and curvature has collectively contributed to the occurrence of landslides in the study area.

Keywords: ***Topographical control, landslide, Thuligad watershed, Farwestern province***

INTRODUCTION

Landslides are regarded as the most consequential and destructive phenomena occurring in mountainous areas worldwide. Mountainous regions exhibit a susceptibility to mass movements as a result of both conditioned and triggering variables (Zhang et al., 2016; Hasegawa et al., 2009). Precipitation, seismic activity, geological condition, topographical attributes and land use act as external catalysts for mass movement (Bhandari and Dhakal, 2018; Tsou et al., 2018; Gerrard 1994; Hasegawa et al., 2009; Zhang et al., 2016; Dahal et al.,2008;

Bhandari and Dhakal, 2019; Bhandari and Dhakal, 2021). Intense precipitation frequently correlates with the initiation of landslides, particularly during the peak monsoon season from June to September in Nepal (Bhandari and Dhakal, 2021; Timalsina and Bhandari, 2024). The interplay of geological conditions, rock weathering, soil erosion, soil moisture, and topographical variables plays a significant role in the dynamics of slope instability (Bhandari and Dhakal, 2018; Bhandari and Dhakal, 2021; Tsou et al., 2018). The impact of human activities, particularly the unrestrained expansion of road networks, and the explosive techniques employed in tunnel construction, and the lack of regulation in agricultural practices on sloped terrains, has been identified as significant factors leading to the recent occurrences of shallow landslides in the Nepal Himalaya (Dahal, 2014; Chamlagain and Dangol, 2022; Thapa et al., 2023; Sharma et al., 2025; McAdoo et al., 2018).

Landslides occur with greater frequency in mountainous regions, causing significant property damage and resulting in fatalities and injuries in many mountainous areas of the developing world, especially in Nepal (Froude and Petley, 2018). Numerous authors have meticulously documented the challenges posed by landslides in the Siwalik and Lesser Himalaya regions of Nepal. Rock avalanches and snow avalanches represent significant hazards in the Higher and Tethys Himalaya region of Nepal. Landslides are becoming more frequent and widespread in the Lesser Himalaya region of western Nepal (Manchado et al., 2021). The regions of Doti, Kailali, Baitadi, and Dadeldhura in Nepal exhibit numerous noteworthy and substantial landslides that have yet to receive comprehensive examination. Topographical data are employed by numerous researchers to assess landslide susceptibility; however, the examination of topographical studies and their correlation with landslides remains limited. The body of work concerning landslide research in Nepal reveals a notable lack of focus on bivariate susceptibility analysis (Regmi et al., 2014; Dahal et al., 2012; Pokharel and Bhandari, 2019; Thapa and Bhandari, 2019; Bhandari et al., 2024), in addition to quantitative assessment and the dynamics observed across various spatial and temporal scales (Bhandari and Dhakal, 2021; Manchado et al., 2022). Nonetheless, there exists a paucity of research exploring the implications and underlying factors, such as precipitation acting as a catalyst and the conditions of the soil (Mugagga et al., 2012; Knapen et al., 2006). The configuration of land surfaces is a fundamental attribute that plays a pivotal role in the likelihood of landslide events (Bhandari and Dhakal, 2019). Nugraha et al. (2015) suggested that the geomorphometric features of terrestrial surfaces are significantly linked to the distribution of landslides. Fernandes et al. (2004) and Broothaerts et al. (2012) have highlighted the significance of investigating the influence of topography on the landslide phenomenon. Giuseppe et al. (2016) contend that the stability of slopes is influenced by a reduction in soil suction across the watershed during precipitation events, in conjunction with increased water pressures that build up in concave areas, where water is directed through saturated subsurface flows as a result of topographical characteristics.

Hung et al. (2018) observed that landslides primarily occurred on steep slopes exceeding 35° within V-shaped inner gorges, as well as on geologically influenced steep slopes, including the scarp slopes of mountain ridges and terrace scarps. Their findings revealed that landslides occur on slopes shaped by topographic and litho-structural factors. The topographic characteristics of hill slope formation and the contributing area have a profound impact on the geographical distribution of landslides. The characteristics of the terrain, including hill slope, aspect, elevation, and curvature, play a significant role in the occurrence of landslides in the hilly regions of Nepal (Bhandari and Dhakal, 2019a). The primary factors influencing landslides encompass the topographical features, especially within the vulnerable and delicate area of the Siwalik Hills

(Bhandari and Dhakal, 2020). Shallow landslides are primarily influenced by topographical features, notably the slope gradient, which is a particularly sensitive factor, as well as lateral concavity (Hennrich and Crozier, 2004). The influence of topography on slope stability is profound; however, the majority of stability models predominantly consider only the slope angle as the relevant topographical variable (Talebi et al., 2008).

The challenging landscape significantly influences the progress of society in the western region of Nepal. In the Far-Western Region, a significant 45.6% of the population resides in poverty (ADB, 2017) and experiences restricted access to essential services (CBS, 2016). Traditional cultural frameworks, intricately associated with religious beliefs and customs, significantly hinder progress (UNFCO, 2012). The demographic patterns observed in the examined region have demonstrated one of the most significant relative surges in Nepal over the last two decades (Worldpop, 2020). This advancement has resulted in significant growth of agricultural areas on steep slopes and the enhancement of infrastructure. The expansion of the road network is particularly noteworthy, frequently linked to inadequate engineering practices (Sudmeier-Rieux et al., 2019). In this context, the configuration of the terrain plays a crucial role in the manifestation of landslides. This study investigates the influence of topographical parameters on landslide occurrences in the Thuligad watershed of Far-Western Province, Nepal

Study area

The study area is located within the Sudurpashchim Province, formerly known as the Far-Western Development Region of Nepal (Fig. 1). The area includes the Thuligad watershed within the Karnali sub-basin, spanning an area of 872.66 km^2. The elevation of the study area ranges from 252 to 2825 meters above sea level. The study area is situated within the Doti and Kailali Districts of Sudurpaschim Province, Nepal.

Geology and Geomorphology

The region is composed of two distinct geological sequences: the Sub-Himalayan (Siwalik) sequence and the Lesser Himalayan sequence (Fig.2). The geological map of the Thuligad watershed in the Siwalik region was developed in the field, although a comprehensive geological map of the Lesser Himalayan sequence is lacking. The southern, southwestern, and western regions of the study area are defined by the Siwaliks zone, which features extensive fragile sedimentary successions of mudstone and sandstone, characterized by upward coarsening sequences (Gansser, 1964). The main boundary thrust (MBT) delineates the separation between the Siwalik and Lesser Himalayan zone, running parallel to the Thuligad River. The region is profoundly shaped by tectonic movements and vigorous rock weathering mechanisms. The Siwalik group within the study area is categorized lithologically into two formations: Lower Siwalik and Middle Siwalik, arranged in ascending order according to their lithology (Fig. 2). The study area encompasses two primary thrusts: the Main Boundary Thrust (MBT) and the Thuligad Thrust (TT). A significant number of landslides have occurred on the steep slopes surrounding the thrust region. The Main Boundary Thrust region is highly susceptible to landslide in the Nepal Himalaya (Paudyal and Maharjan, 2022). Some of the representative landslides near the thrust zone are shown in the Figure 3. The Lower Siwalik is composed of fine-grained sandstone and mudstone, with thicknesses varying from ten centimeters to meters, occurring in nearly equal proportions (Dhital, 2015). The Middle Siwalik is characterized by substantial bedded, multistoried, pepper and salt sandstone, interspersed with notably thick gray mudstones. The majority of the sandstones exhibit a dark grey-green hue, characterized by a medium to fine grain size, and are interspersed with subtle gray to gray-green shale (Dhital, 2015). This study area comprises a significant quantity of dolomite and limestone at the upper boundary of the Middle Siwaliks. The Lesser Himalaya within the study

area is composed of limestone and low-grade metamorphic rocks, including pink dolomite, grey slate, phyllite, and quartzite.

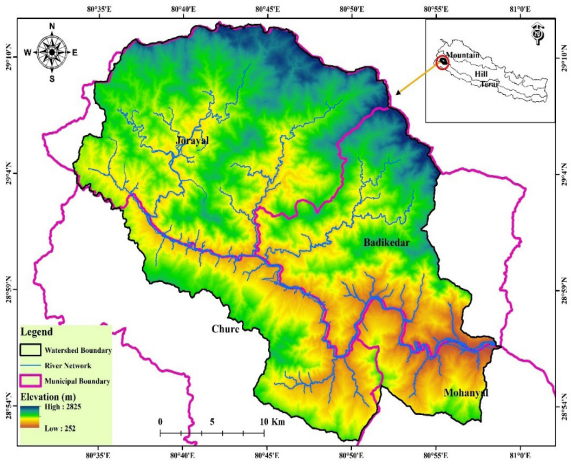

Fig.1: Location map of study area

The morphology of area is dynamically changing due to landslides, frequent flash floods and debris flows (Dhital, 2015). The north eastern part of the region is characterized by steep slope, which attains the highest elevations and exhibits the steepest topographies.

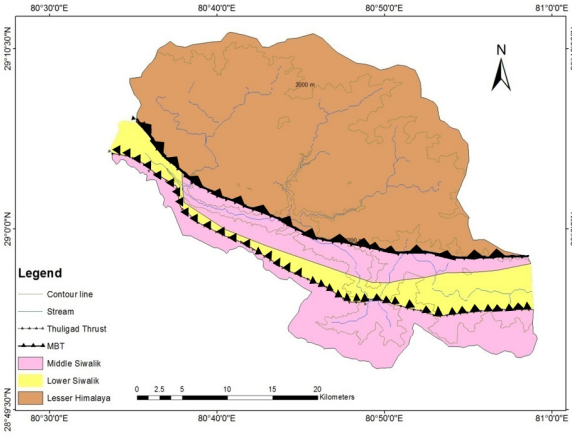

Fig. 2: General geological map showing the Siwalik and Lesser Himalayan sequences separated by Main Boundary Thrust (MBT)

CLIMATE

Temperature and precipitation fluctuate according to both seasonal changes and elevation. Data from meteorological and hydrological stations show that the average annual temperature in the Thuli Gad watershed is 23°C. The average maximum and minimum monthly temperatures vary from 5°C to 24°C during winter and from 21°C to 40°C in summer. The watershed exhibits a climatic gradient from subtropical conditions in the south to alpine characteristics in the north, with elevations ranging from 252 meters in the southern areas to 2825 meters in the northern regions. The study area commences in the Siwalik region and transitions through hilly terrain into mountainous regions. The watershed experiences a total annual rainfall of approximately 3017 mm, with an average of 2160 mm per year.

METHODS

Landslide inventory

The landslide inventory map of the study area was prepared by using utilizing satellite imagery sourced from Google Earth and Landsat having 30 m resolution, considering both spatial and temporal factors. The overlapping imagery was eliminated, characterized by significant cloud cover, blurring effects, or darkness, to enhance the interpretation of features related to landslides. The identified landslides were delineated by the polygon extending from the scar to the toe area. The generated traced map was acquired using GIS for spatial analysis, topological correction, and feature post-processing (Fig. 4). The area and summary statistics of the landslides were derived from the GIS analysis. Several field visits and onsite mapping were conducted to clarify the confusion sites.

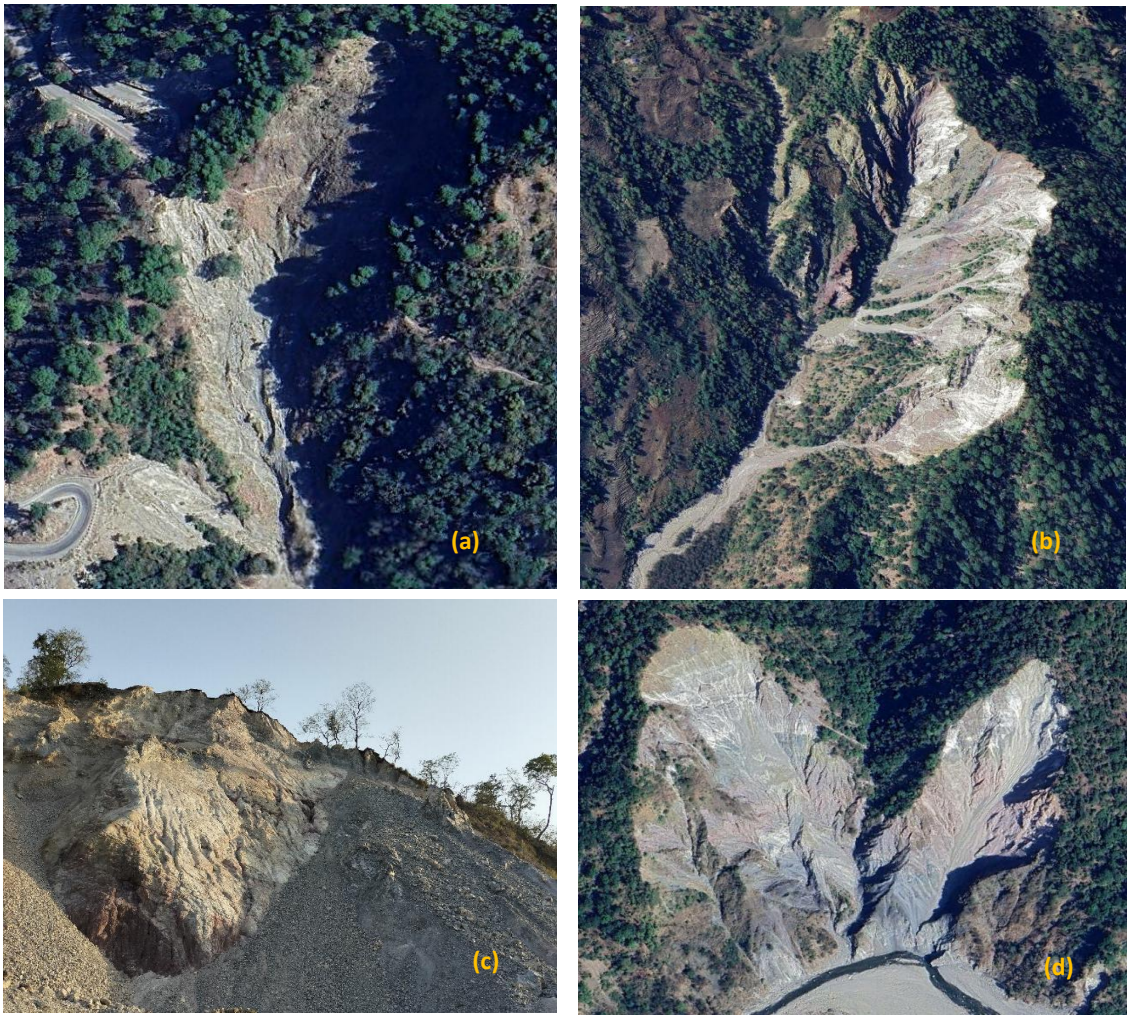

Fig.3: The four major active landslides occurred on the steep slope near the thrust zone

Field observation

A field survey was executed in the study area to validate the inventory map developed through satellite imagery analysis. A GPS (Garmin 60sx) was utilized to georeference and validate the landslide scars that were not discernible from the imagery. The locations of the landslides were represented through unique polygons and/or points that correspond to the scarps of the movements illustrated on the map. The observations conducted during fieldwork focused on slope gradient, position, curvature, and aspect, aiming to evaluate the role of topography as a significant factor in the incidence of landslides within the research area. The ancient scars presented a formidable challenge for classification, owing to the ambiguous shapes resulting from erosion and the encroachment of vegetation. A thorough analysis of the scars and depletion zones was undertaken to ensure accurate mapping. The interviews were conducted with certain key individuals to obtain additional insights concerning the date, scope, and nature of the movement.

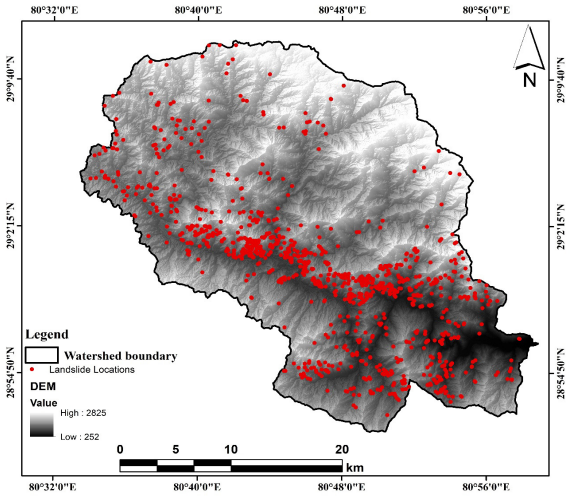

Fig. 4: Landslide inventory map of the Thuligad watershed

Topographical factors

A Digital Elevation Model (DEM) with a resolution of 12.5 m, obtained from the ALOSPALSAR website, was used to create an influencing factor map for landslides. The topographical factor maps such as slope, aspect, Topographic Wetness Index (TWI), curvature, and Stream Power Index (SPI) were obtained from the spatial analyst tool of ArcGIS.

Slope

The slope serves as a pivotal element, significantly influencing the occurrence of landslides. Slope failure generally arises from variations in shear stress along the slope, which are affected by gravitational forces. On any slope, there exist forces that facilitate movement downwards, alongside counteracting forces that impede such motion. Diverse forms of slope movements identified stem from conditions that compromise the stability of the slope, ultimately leading to displacement (Karimi et al., 2020). Mass wasting or sliding events occur with greater frequency on steep terrain in contrast to gentle slopes. The slope angle map was produced automatically in ArcGIS 10.8 utilizing a digital elevation model (DEM) with a grid cell size of 12.5 m. This map is categorized into five distinct ranges: 0-15, 15-30, 30-45, 45-60, and exceeding 60 degrees, reflecting the variations in terrain morphology (Bhandari et al., 2024) (Fig.5).

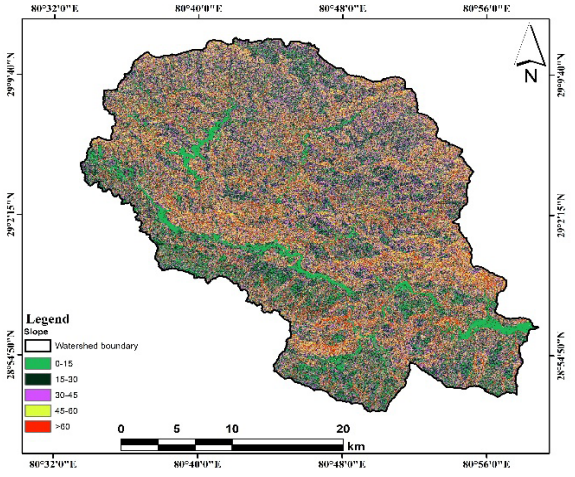

Fig. 5: Slope map of the Thuligad watershed, Far western province, Nepal

Aspect

Soil moisture patterns and regional physiographic trends are relevant to this feature. Its effects on weathering, plant life, and root growth are amplified by the way it changes the direction of evapotranspiration and frontal precipitation (Bhandari and Dhakal, 2020). Assessing geomorphologic stability is greatly influenced by slope aspect, which controls a variety of environmental variables including soil moisture, rainfall intensity, received radiation, and wind (dry and wet) (Huang, 2015). Based on the classification of natural breaks, the aspect map sorts aspects into nine groups: Flat, North, Northeast, East, Southeast, South, Southwest, West, and Northwest (Fig.6).

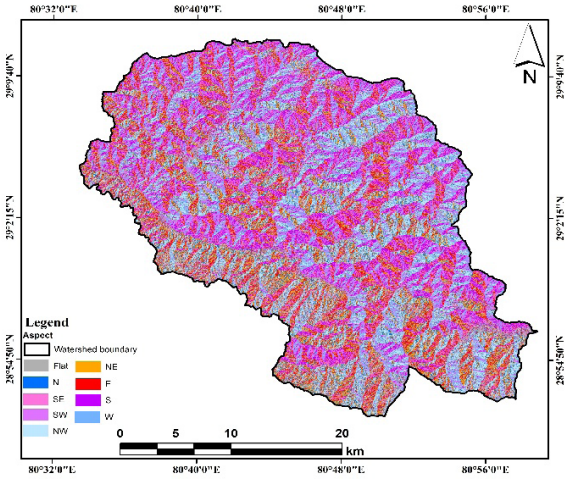

Fig. 6: Aspect map of the Thuligad watershed, Far western province, Nepal

Plane and Profile Curvature

The curvature is considered as the slope of the slope or second darivative of the slope. The Curvature tool available in the Spatial Analyst or 3D Analyst toolbox facilitates the creation of three distinct curvature: an output curvature, a profile curvature, and plan curvature. Profile curvature is aligned with the direction of the maximum slope. A negative value signifies that the surface exhibits upward convexity at that cell. A positive profile indicates that the surface is upwardly concave at that cell. A value of zero indicates that the surface is linear Profile curvature influences the acceleration or deceleration of flow over the surface. Both plane and profile Curvature values were classified into three classes (concave, flat (linear) and convex) based on the obtained raster class value (Fig.7 & 8). The area consists of more or less equal pixels of each curvature however, flat curvature seems dominant due to color contrast and uneven distribution of the curvature.

Topographic wetness index (TWI)

The TWI map was generated using GIS software and calculated with the formula TWI = ln (A / tanβ), utilizing a Digital Elevation Model (DEM) from ALOSPALSAR with a resolution of 12.5 meters. The thematic map displays the Topographic Wetness Index (TWI) values across a watershed, categorized into five ranges using the natural breaks classification method to indicate varying levels of soil moisture and potential for water accumulation. The TWI values are divided into the following ranges: -0.9 - 2.8, 2.8 - 4.8, 4.8 -7.5, 7.5-11.8, and 11.8- 26(Fig.9).

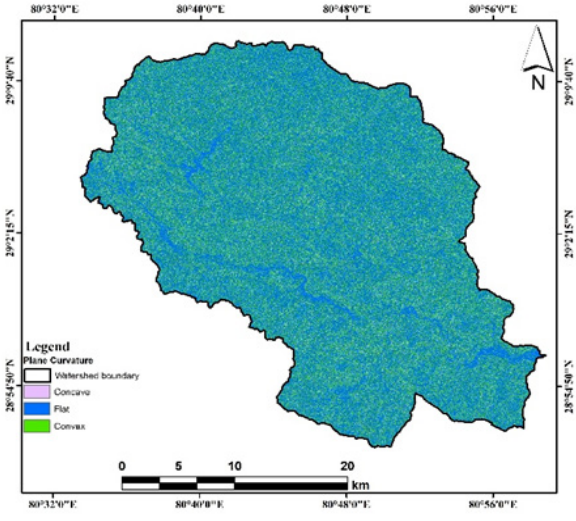

Fig. 7: Plan curvature map of the study area

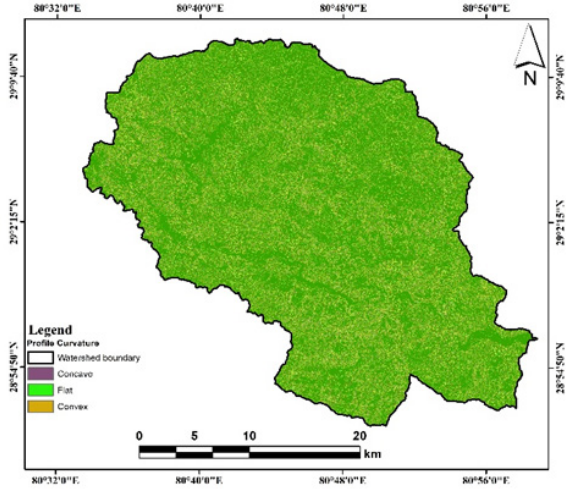

Fig. 8: Profile curvature map of the study area

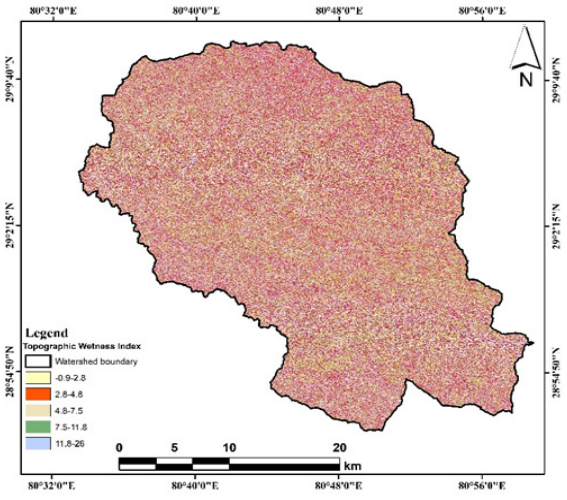

Fig. 9: Topographical wetness index map

Stream power index

The Stream Power Index (SPI) quantifies the erosive capacity of flowing water. The SPI is determined by the slope and the contributing area. SPI estimates potential locations for gully formation within the landscape. The thematic map displays the SPI values across a watershed, categorized into five ranges indicate varying levels of erosive power of flowing water. These colors help visualize areas within the watershed that experience different levels of erosion and sediment transport, with red indicating the lowest SPI and blue indicating the highest SPI (Fig. 10).

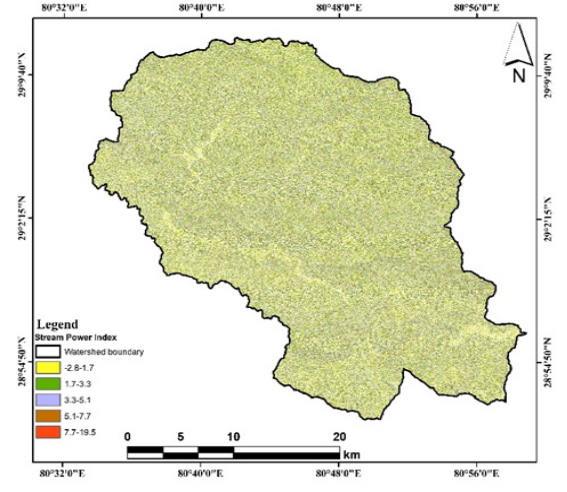

Fig. 10: Stream power index map of the study area

Landslide analysis

Various authors applied statistical index model for finding the correlation between landslides and causative factors (Cui et al., 2017; Firomsa et al., 2019, Cheng et al., 2022). The statistical index is a bivariate statistical method developed by van Westen (1997) for assessing landslide susceptibility (Pardeshi et al., 2013). This method defines a weighted value for a parameter class as the natural logarithm of the landslide density within the class divided by the landslide density throughout the entire map (Pradhan et al., 2012). Mezughi et al. (2011) demonstrate that the outcome generates a cross table, which is subsequently employed to calculate the density of landslides for each parameter class, with each causative or thematic map being separately overlaid and intersected with landslide inventory data. This study employs this method to establish the correlation between landslide occurrences and slope factors, thereby assessing the influence of topographical elements on landslide events. Pradhan et al. (2012) state that SIM is computed using the equation

$$Wij = \ln\left(\frac{fij}{f}\right) = \ln\left(\frac{\frac{Lij}{Aij}}{\frac{L*}{A*}}\right)$$

Where, Wij represents the weight value of category j of factor i, fij represents the landslide density in class j of factor i, f represents the landslide density in the entire study area, Lij represents the number of landslide units in class j of factor i, Aij represents the number of units contained in class j of factor i, L∗ represents the total number of landslide units in the study area, and A∗ represents the total number of units in the study area.

The Wij value signifies the correlation between the causal factors classification and landslide distribution.

So that this statistical index model is used in this study to identify the correlation between the classes of factors with the landslide density. A high weight value for a class implies a significant association between the causative elements and prior landslides, whereas a low weight value signifies a weak relationship. In the current investigation, Wij values of causal factors were computed. In the absence of landslide occurrences within a causative factor class, Wij is assigned a value of zero (van Westen, 1997). The causative factor maps were overlaid using landslide inventory data. The Wij values for the causative factor classes without relationships were not weighted (zero values were assigned).

RESULTS

The sub class of topographical factors and number of landslide as well as the area of landslides were obtained from the summary statistics of ArcGIS. The research investigates landslides in the Thuligad watershed through satellite imagery and field visits, identifying 1156 landslides in total.

Topographical distribution of landslide

We acquired the statistical index values and landslide density for each class of factors. Table 1 presents the SI value and landslide density for each slope class where the SI value rose with the steepening of the slope. Only 47% of the area has a slope over 30 degrees, although it covered roughly 73% of landslides area on it. Only 15% of landslides area lied on slopes between 15 and 30 degrees, while only 2% occur on slopes less than 15 degrees. The Figure 11 illustrates the percentage of area occupied by slope class and landslide. On slopes over 60°, the density of landslides is highest however, the landslide percentage in total is highest between the slopes 30° to 45°. The landslide percentage on the slope greater than 60° is lowest indicates that the landslide number decreased on the slope greater than 45° however, the overall result signifies that the percentage of land having slope greater than 45° is less in the study area. In case of landslide density, it is highest on the slope greater than 60°. This result indicates that the landslides are mainly controlled by slope in the study area. Similarly, the statistical index values increased with increasing the slope. The landslide intensified as the slope increased. Steep slopes typically reduce the incidence or extent of landslides, as the steep region may be smaller than other classifications. However, density analysis can yield a more accurate assessment of slope stability in landslides. The area of the slope class is smaller than other classes, but the area of the landslide is larger when considering the landslide class area ratio. The percentage of landslide density has markedly risen with the elevation of the slope. The four major landslides that are located in the same regions and have a similar rainfall pattern and geology but slope angle exceeded 30° are shown in the figure 12. The mechanisms of landslide initiation are comparable on slopes that are similar.

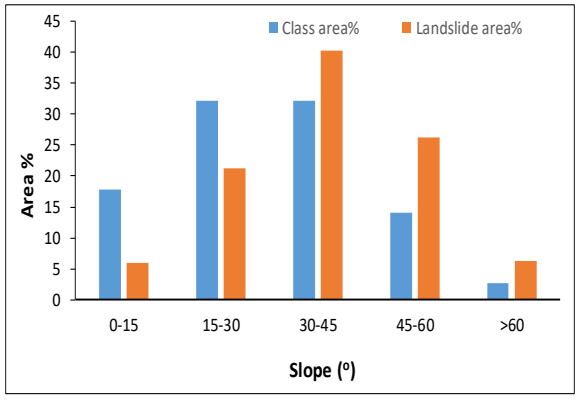

Fig. 11: The distribution of slope class percentage and landslide percentage on the particular classes

The topographical wetness index demonstrated an inverse relationship with landslides. The SI value and landslide density decreased with an increase in TWI value. Increased TWI levels correlate with a reduction in the frequency of landslides. In the lowest TWI class (-0.9 to 2.8), the SI value is 0.061; in contrast, in the highest TWI class (7.5 to 11.8), the SI value is -0.004.

The results indicate that the southern, southeastern, and southwestern aspects exhibit a higher susceptibility to landslides. The SI values for the southern, southeastern, and southwestern aspects surpass those of the other aspects. The north, northeast, and northwest aspects show significantly lower SI values, suggesting a decreased susceptibility to landslides in the studied area. Concave and convergent curvatures exhibit a greater susceptibility to landslides, attributed to their significantly elevated SI values in comparison to convex, divergent, and planar surfaces. The results of plan and profile curvature are similar. The SPI range of (-2.8-1.7) corresponds to a SI of -0.001; the range of (1.7-3.3) has a SI value of 0.537; the range of (3.3-5.1) shows a SI of 1.105; the range of (5.1-7.7) indicates a SI value of 1.212; and the range of (7.7-19.5) presents a SI value of 1.751. The SI value has increased in conjunction with the rising SPI.

Number based landslide distribution on the topography

The incidence of landslides escalated with the slope angle, peaked between 30° and 45°, and thereafter diminished beyond 45°(Fig.13). The landslide distribution curve is more likely to follow a normal distribution.

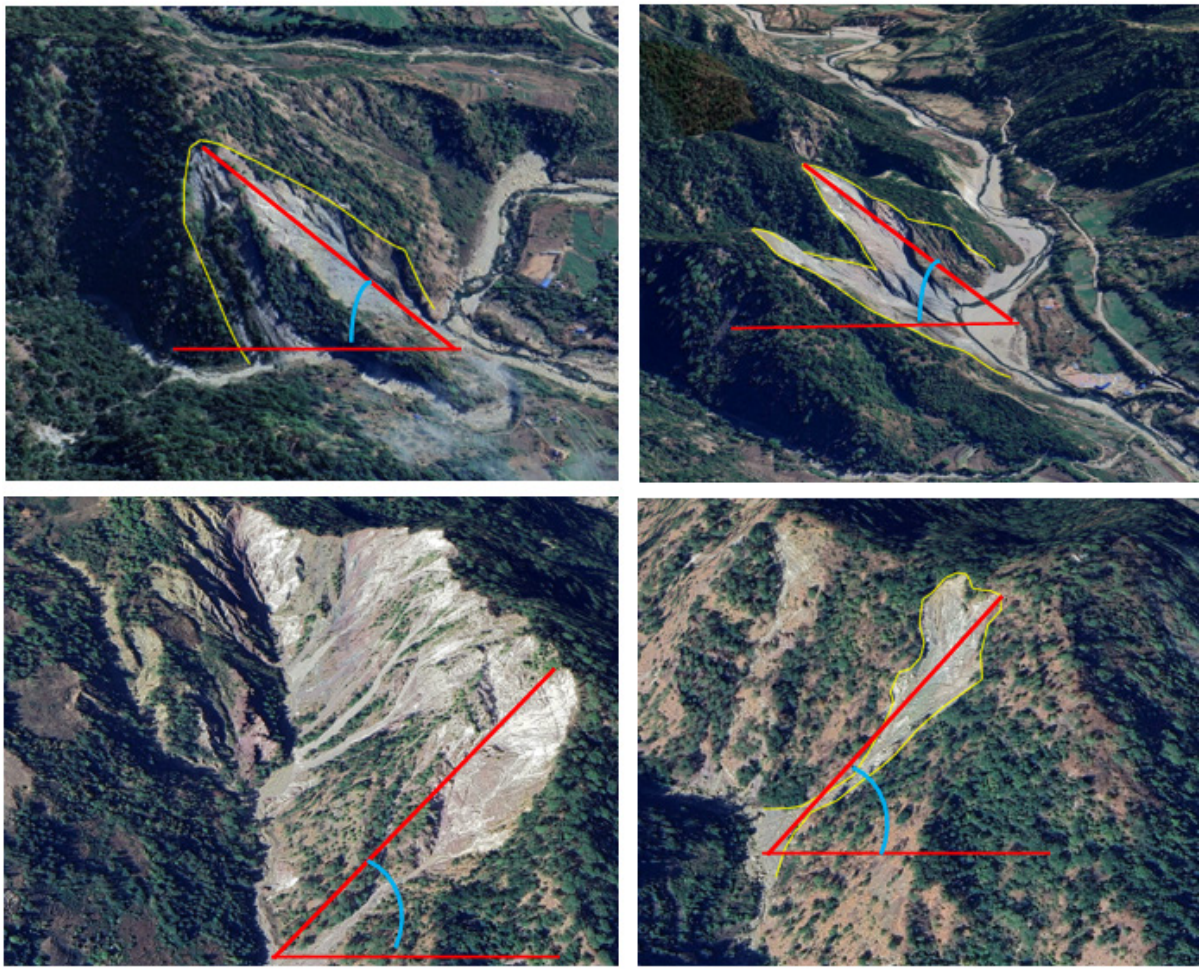

Fig.12: The slope control landslides form four different locations in the study area

Table 1: Landslide density and SI value in the different factors classes

Factors	Class	Class pixel	Landslide pixel	Landslide density	Statistical Index
Slope	0-15	8334816	6647	0.0081	-0.481
	15-30	15033101	23859	0.0163	-0.180
	30-45	14995626	45042	0.032	0.096
	45-60	7032186	29365	0.042	0.240
	>60	1268508	7095	0.056	0.367
	(-0.9-2.8)	18987256	52282	0.245	0.061
TWI	2.8-4.8	17039500	33452	0.195	-0.086
	4.8-7.5	7446831	19077	0.180	-0.029
	7.5-11.8	2698667	6424	0.145	-0.004
SPI	(-2.8-1.7)	25256789	43366	0.0017	-0.001
	1.7-3.3	9778201	23787	0.0024	-0.537
	3.3-5.1	5866302	19903	0.0033	1.105
	5.1-7.7	3845670	14267	0.0037	1.212
	7.7-19.5	1934567	10087	0.0052	1.751
Aspect	North	6576674	6274	0.0493	-0.397
	Northeast	6055454	5659	0.0483	-0.408
	East	5509576	12594	0.1183	-0.022
	Southeast	5864100	22028	0.1944	0.193
	South	5904078	26742	0.2344	0.276
	Southwest	5879987	18513	0.1629	0.117
	West	5368486	10655	0.1027	-0.080
	Northwest	5505882	9543	0.0897	-0.142
Profile curvature	(-531- -22)	3450803	11471	0.0033	0.141
	(-22-11)	34997953	75231	0.0021	-0.047
	11-686	8249477	15306	0.003	0.106
Plan curvature	(-841.8--21.7)	2101993	7958	0.0037	0.1981
	(-21.7-3.8)	28850891	64875	0.0022	-0.0281
	3.8-785.7	15745349	39175	0.0024	0.0158

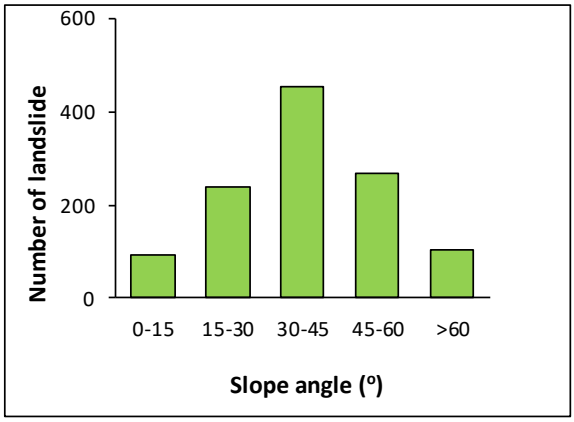

Fig.13: Distribution of landslide on the of slope classes

The incidence of landslides is significantly higher on concave slopes compared to convex and planar slopes (Fig.14).

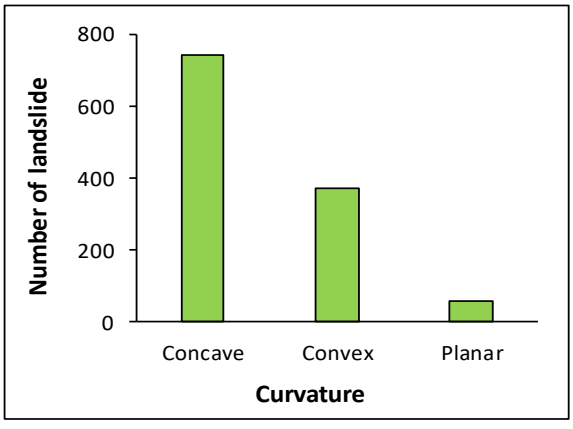

Fig.14: Distribution of landslide on the curvature

Likewise, the incidence of landslides on the southern side is markedly greater than that on other aspects.

Both the field observation and model-based results exhibited comparable outcomes. Likewise, the decadal temporal inventory map indicated that the frequency of landslides is greater on slopes ranging from 30° to 45°.

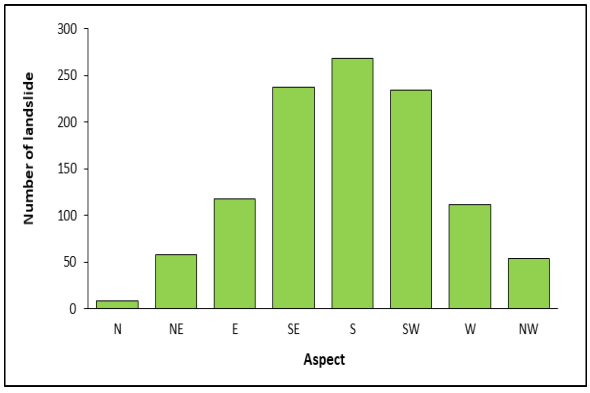

Fig. 15: Distribution of landslide on the aspect

Temporal slope distribution

The overall number of landslides from 2010 to 2024 was derived from the temporal landslide inventory mapping over three years. The temporal inventory maps were superimposed on the slope map in ArcGIS. The total number of landslides was quantified for the specific slope pixel, hence determining the landslide count for that slope. The temporal distribution of landslides on the slope revealed that the frequency of landslides is greater on slopes ranging from 30° to 45° across various years. Every three years, the incidence of landslides is markedly higher on slopes between 30° and 45°, and considerably lower on slopes below 15° and above 60°. Nonetheless, the results of landslide density indicated that it is increased on slopes greater than sixty degrees. The frequency of landslide events increased with the steepening of the slope. The surface area above the slope class 60° is smaller compared to other slope classes. The area of the slope class 30° to 45° is significantly greater in the study area so that the landslide distribution is also greater. The year wise distribution of landslide form 2010 to 2024 is shown in the figure 11.

Size based slope distribution

Landslide sizes were categorized into five classifications: very small, small, medium, large, and very large (Bhandari and Dhakal, 2019). The size of the landslides were determined based on the area.

Bhandari and Dhakal (2019) classify landslides as follows: less than 100 m² is very small, 100 to 1,000 m² is small, 1,000 to 10,000 m² is medium, 10,000 to 100,000 m² is large, and greater than 100,000 m² is very large. The total number of landslides across various slopes was evaluated, and the distribution of landslides according to their sizes within specific slope classes is illustrated in Figure 16.

The medium-sized landslide is prevalent on slopes greater than 15 degrees. Very small landslides are predominantly observed on the slopes less than 15 degrees. Distribution of both very large and very small landslides are limited on slopes between 30 and 45 degrees. A higher incidence of very large landslides was observed on slopes greater than 60°. A significant number of landslides occurred solely on slopes exceeding 30 degrees; however, the majority of large sized landslides are found on slopes greater than 60 degrees.

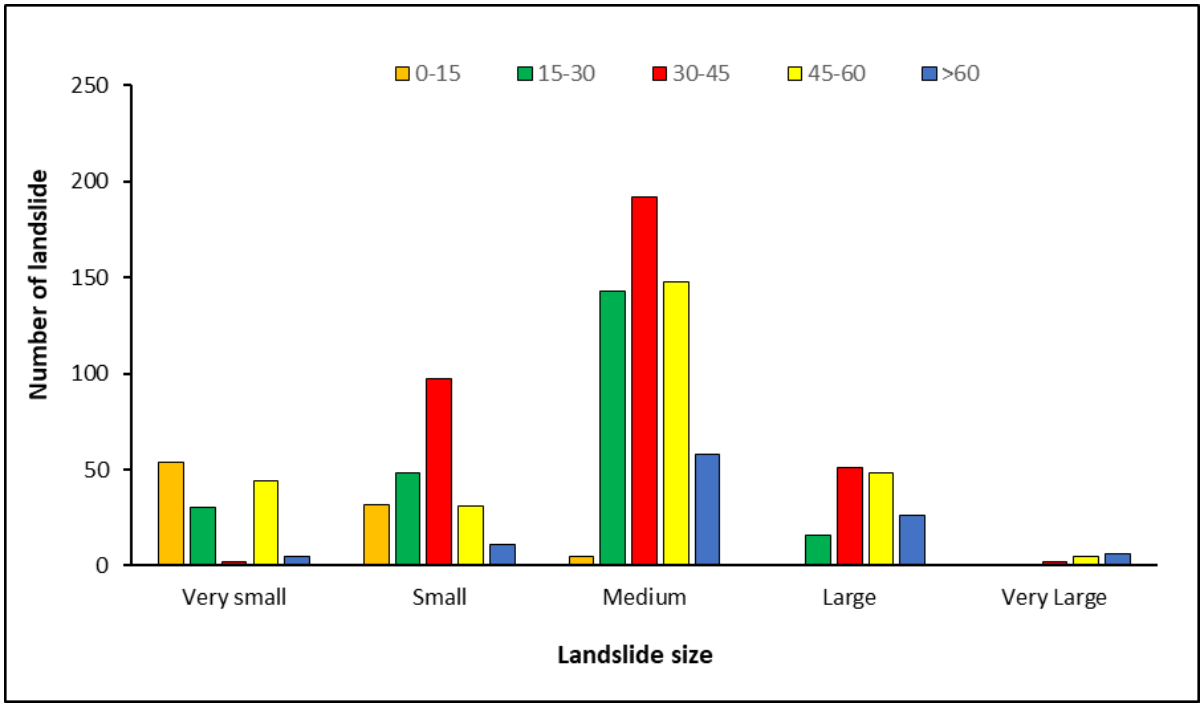

Fig.16: Size based landslide distribution on the slopes

A notably higher frequency of very small landslides was observed on slopes ranging from 30° to 45°, while the occurrence of large and very large landslides is more prevalent on slopes exceeding 45°. The findings indicated that the slope determines the extent of the landslide.

DISCUSSION

The presence of little streams on the slope, generated by rainwater drainage, indicates the number of dissections in the natural slope. The drainage pattern of these streamlets is dendritic. In the study region, haphazard road construction is a major issue that contributes to soil erosion and landslides. The Budar-BP Nagar highway is located in the Siwalik region and traverses the highly fractured dolomite and slate that mark the boundary between the Siwalik and the Lesser Himalaya. Forest fires are another major problem

in the study region, so the deforestation issue is growing. Vegetation on slopes no longer serves its protective purpose due to deforestation and changes in land use caused by urban development. Deforestation and unmanaged agriculture on the steep slope are causing a huge amount of soil loss. Loss of soil-stabilizing root systems can make erosion worse and landslides more likely (Singh et al., 2021). Changes in land use within the research area may have significantly impacted slope stability. Unregulated development activities, particularly road construction and building settlement, accelerated this shift in land use.

The stability of slopes is greatly affected by their shape, gradient, and configuration, which are measured and analyzed in slope morphometry. Slopes in the Thuligad watershed generally face south and have an average angle of 27 degrees. Erosion and the formation of numerous rill and gullies are consequences of first and second-order streams cutting over the slopes during times of high discharge during the wet seasons. Between 250 and 1850 meters is the altitude of the areas. Gravitational forces acting on soil and rock are directly affected by the slope angle, according to studies. Saturated conditions, in particular, increase the risk of failure as the slope angle rises (Ghosh et al., 2020). Landslides tend to be more common on steeper slopes. A concave pattern is visible on the slope. Failures occur as a consequence of increased pore pressure caused by water collected on the concave slopes (Sharma et al., 2019). Similarly, the region's small hills, valleys, and overhangs can change the way silt accumulates and drains, which can affect the likelihood of landslides. Slope collapse and increased saturation can occur when water collects in nearby concave (Lee et al., 2022). Microclimates, shaped by the slope aspect, impact soil moisture levels and plant growth. While the majority of the area's slopes face northeast, southeast, and southwest, the number of landslides is highest in the southeast, southwest, and southwest directions. Furthermore, the presence of several springs, seepages, and puddles on the slope suggests that the water table is quite shallow in the area. The shear strength of the materials that constitute the slope was greatly diminished as the slope angle increased, which in turn affected the soil erosion and landslide. In a similar vein, increasing the slope angle affected surface runoff and weathering by increasing the shear stress of the slope materials. Additionally, landforms have been significantly damaged and landslides have increased due to the careless construction of roads on the geologically fragile slope. Because it alters natural drainage patterns and adds soil stress, road development on a slope can destabilize the slope. Landslides can occur when excavation techniques and heavy machinery are used on slope surfaces, as they can disturb the geological stability (Gupta et al., 2021). Soil surface conditions have been worsened by recent changes in vegetation cover, which have increased insufficient water pressure, undermined slope stability, and made rainwater interception more difficult.

Bhandari and Dhakal (2019b) conducted a study on the influence of topography on gully-type landslides within the Malai River catchment in Nepal, emphasizing the considerable impact of the topographical factor "T" on landslide occurrences. In that work, the authors further elucidated the synergistic influence of slope and geological factors on the initiation of landslides. Bhandari et al. (2024), Thapa and Bhandari (2019), Pokharel and Bhandari (2019), Ayer and Bhandari (2024), Paudyal et al. (2024) and Paudyal and Maharjan (2023) established a correlation between topographical factors and landslide pixels. Bhandari and Dhakal (2020) examined the correlation between landslides and topographical factors within the Babai River watershed in Nepal, highlighting the substantial influence of topography in the occurrence of landslides. Nakileza and Nedala (2022) studied topographical influences on the landslide characteristics of Mt. Elgon, Uganda and highlighted the outcome as the topography play

significant role to control landslide mechanism. The authors further highlighted the relation between the slope and hydrological processes so that the development of the landslide becomes faster in the weak geological conditions. Knapen et al. (2006) highlighted that slope segments that are steep, plan concave, and oriented to the prevalent rainfall direction are the most sensitive to mass movement. The movement occurs at a particular distance from where the water divide. This was the case for slope segments that meet all of these criteria.

The distribution of landslides is significantly related to land surface and morphometric features, according to Nugraha et al. (2015). In the Tinalah watershed, for example, they found that landslides typically occur at an elevation greater than 400 m.a.s.l., on slopes that are 20 degrees, oriented east to west, and with a flat curvature. According to them, the topographical factors show the effects together and control the landslide mechanism. Dahle et al. (2011) studied the spatial distribution of debris-slides and noted that the spatial distribution of debris slides are determined by the aspect, slope angle, stream density, plan curvature, and altitude. According to research conducted by Nseka et al. (2019), a greater frequency of landslides occurred on slopes ranging from 25 degrees to 35 degrees in the western highlands of Uganda. According to Bizimana and Sonmez, (2015), the locations that are most susceptible to landslides are those that have slope angles that are greater than 14 degrees on convex slopes and greater than 41 degrees on concave slopes. In the Democratic Republic of the Congo, Depicker et al. (2018) found that the slope threshold was 24.8 degrees, however in South Africa, slopes ranging from 21 degrees to 30 degrees had the highest landslide frequency. On the other hand, Zhuang et al. (2015) discovered that the largest density of landslides, specifically 51.81 percent, was found in a higher slope range of 15–40 degrees. Shear forces that act on the hillside are controlled by the slope gradient (Silalahi et al., 2019), and as a result, slopes that are steeper are more likely to be affected by these forces. In the present study, the result shows that the landslides are mostly controlled by slope. Paudyal et al. (2021) noted that the southern aspect having slope greater than 20o is more susceptible to cause landslide in the terrains of Farwestern Nepal. Zhuang et al. (2015) reported that landslide occurrences are numerous at areas with convex and concave surfaces. According to Regmi et al. (2014) debris flows are more likely to take place in areas of topographic convergence that are covered by unconsolidated deposits. The majority of rock slides take place on slopes that are steep and convex to planar. Many researchers reported that the concave curvature is highly prone to landslide in the Himalaya. The flow type landslide is very common on the concave slope. The topographic wetness index (TWI) exposes the diversity and complexity of the topographic surface of landslides. It does this by identifying zones of preferential drainage within the landslide body as well as comparatively dry areas within its limits. Low TWI values are generally observed in the top regions of landslides, particularly steep head. For landslides that are created in slope hollows and are launched as shallow slides, the relationship between the depletion zone and low TWI is less obvious. Timalsina and Bhandari (2024), along with Bhandari et al. (2024) and Ayer and Bhandari (2024), have documented the inverse relationship between TWI class and landslide pixels. Their findings indicate that the landslides pixel diminishes as the TWI value rises.

The SPI measures the erosive capacity of flowing water by considering both the drainage area and the local slope. Moore et al. (1993) illustrated the efficacy of SPI in delineating areas of concentrated water flow and erosion potential, which has a direct impact on landslide hazard assessment. Tarolli et al. (2012) demonstrated a significant correlation between SPI and the initiation of channels as well as erosion hotspots in steep mountainous regions due to fast flowing water. Reichenbach et al. (2018) demonstrated through a comprehensive

global review that SPI is often incorporated into data-driven models of landslide susceptibility. A multitude of researchers have underscored the affirmative relationship between the stream power index and landslides occurring on slopes. Timalsina and Bhandari (2024) elucidated the robust correlation between SPI and landslides at the catchment scale because stream power index is one of the major hydrological factor to cause landslide. This study reveals a significant correlation between the SPI and landslide occurrences within the examined region. Elevated SPI values manifest at the confluence of steep slopes and extensive contributing areas. The characteristics of these locations frequently exhibit elevated water discharge and velocity, thereby augmenting the potential for erosion. The erosion of slopes at their base, commonly referred to as toe erosion, caused by hydrological action of streams can significantly diminish slope stability, potentially leading to the occurrence of rotational or translational landslides. SPI delineates regions susceptible to gully formation, which may develop into more profound incised features. The presence of these gullies serves to concentrate runoff, thereby exacerbating local erosion and compromising the stability of the adjacent slope. In steep catchments, elevated SPI zones may align with the origins of debris flows, particularly following periods of intense precipitation or snowmelt. SPI serves as a valuable tool for modeling the trajectories of debris flow and assessing the potential for sediment yield.

CONCLUSION

This study revealed the impact of topographical factors on triggering landslides within the Thuligad watershed of Sudurpaschim Province, Nepal. The development of the topographical factors map, including slope, aspect, topographical wetness index, stream power index, and plan and profile curvature, was executed using ArcGIS. The results indicate that slope is crucial in landslide occurrence, with a significant increase in landslide density associated with an elevation in slope angle. The gradient between 30 and 45 degrees is most prone to landslides in the research area. The reduction in the statistical index value as TWI rises indicates an inverse correlation between TWI and landslides. The study area has multiple gullies and inclines over 15 degrees, leading to an increased stream power index. The incidence of landslides increased in response to the elevated stream power index. The concave slope demonstrates significant sensitivity in the research area, with a higher incidence of landslides recorded in this terrain relative to the convex slope. The southern aspect, marked by a slope angle more than 30 degrees and a concave contour, resulted in an increase in the SPI. The TWI increases as one nears the hill's base and persists while ascending until its peak. The comprehensive findings suggest that topographical elements together regulate landslide activities. This investigation may aid in comprehending the topography's influence on landslides in analogous places of Nepal. It offers both basic and specialized information regarding slope management for landslides, thus enabling local planners and designers to create roads in a scientific manner.

REFERENCES

ADB, 2017, Country poverty analysis (detailed) Nepal, Asia Development Bank. https://www.adb.org/sites/default/files/linked-documents/cps-nep-2013-2017-pa-detailed.pdf. Accessed 24 June 2020.

Ayer, P. B. and Bhandari, B. P., 2024. Landslide Susceptibility Mapping Using Frequency Ratio and Weight of Evidence Models in Purchaudi Municipality, Baitadi District, Nepal, *Nepal Journal of Environmental Science*, *12*(2), 59-72.

Bhandari, B. P. and Dhakal, S., 2018. Lithological control on landslide in the Babai Khola watershed, Siwaliks zone of Nepal, *American Journal of Earth Sciences*, *5*(3), 54-64.

Bhandari, B. P. and Dhakal, S., 2019a. Evolutional characteristics of debris flow in the Siwalik

Hills of Nepal, *International Journal of Geosciences*, *10*(12), 1049.

Bhandari, B. P. and Dhakal, S., 2019b. Topographical and geological factors on gully-type debris flow in Malai River catchment, Siwaliks, Nepal, *Journal of Nepal Geological Society*, *59*, 89-94.

Bhandari, B. P. and Dhakal, S., 2020. Spatio-temporal dynamics of landslides in the sedimentary terrain: a case of Siwalik zone of Babai watershed, Nepal, *SN Applied Sciences*, *2*, 1-17.

Bhandari, B. P. and Dhakal, S., 2021. A multidisciplinary approach of landslide characterization: A case of the Siwalik zone of Nepal Himalaya, *Journal of Asian Earth Sciences: X*, *5*, 100061.

Bhandari, B. P., Dhakal, S. and Tsou, C. Y. 2024. Assessing the prediction accuracy of frequency ratio, weight of evidence, Shannon entropy, and information value methods for landslide susceptibility in the Siwalik Hills of Nepal, *Sustainability*, *16*(5), 2092.

Bizimana, H. and Sönmez, O., 2015. Landslide occurrences in the hilly areas of Rwanda, their causes and protection measures, *Disaster Science and Engineering*, *1*(1), 1-7.

Broothaerts, N., Kissi, E., Poesen, J., Van Rompaey, A., Getahun, K., Van Ranst, E. and Diels, J., 2012. Spatial patterns, causes and consequences of landslides in the Gilgel Gibe catchment, SW Ethiopia, *Catena*, *97*, 127-136.

CBS, 2016. Annual household survey report 2014-15. Central Bureau of Statistics - National Planning Commission Secratariat, Government of Nepal, UNDP. Thapathali, Kathmandu, Nepal 120 pp

Chamlagain, D. and Dangol, V., 2002. Landslide hazard evaluation in and around the Ilam Hydropower Project, Eastern Nepal Himalaya, *Journal of Nepal Geological Society*, *27*, 131-143.

Cheng, C., Yang, Y., Zhong, F., Song, C. and Zhen, Y., 2022. An optimization of statistical index method based on Gaussian process regression and geodetector, for higher accurate landslide susceptibility modeling, *Applied Sciences*, *12*(20), 10196.

Cui, K., Lu, D. and Li, W., 2017. Comparison of landslide susceptibility mapping based on statistical index, certainty factors, weights of evidence and evidential belief function models, *Geocarto International*, *32*(9), 935-955.

Dahal, R. K., 2014. Regional-scale landslide activity and landslide susceptibility zonation in the Nepal Himalaya, *Environmental Earth Sciences*, *71*, 5145-5164.

Dahal, R. K., Hasegawa, S., Bhandary, N. P., Poudel, P. P., Nonomura, A. and Yatabe, R.,2012. A replication of landslide hazard mapping at catchment scale, *Geomatics, Natural Hazards and Risk*, *3*(2), 161–192. https://doi.org/10.1080/19475705.2011.629007

Dahal, R. K., Hasegawa, S., Nonomura, A., Yamanaka, M., Dhakal, S. and Paudyal, P., 2008. Predictive modelling of rainfall-induced landslide hazard in the Lesser Himalaya of Nepal based on weights-of-evidence, *Geomorphology*, *102*(3-4), 496-510.

Dahl M.P.J., Mortensen, L.E., Jensen, N.H. and Veihe, A., 2011. Magnitude–frequency characteristics and preparatory factors for spatial debris-slide distribution in the northern Faroe Islands, Geomorphology 188(2013):3–11

Depicker, A., Govers, G., Van Rompaey, A., Havenith, H.B., Mateso, J.C.M. and Demitte, O., 2018. Landslides in a changing tropical environment: North Tanganyika-Rift Kivu zones. https://www.researchgate.net/publication/325176935

Dhital, M. R., 2015. Geology of the Nepal Himalaya: Regional Perspective of the Classic Collided Orogen. Berlin: Springer. https://doi.org/10.1007/978-3-319-02496-7

Fernandes, N. F., Guimarães, R. F., Gomes, R. A., Vieira, B. C., Montgomery, D. R. and Greenberg, H., 2004. Topographic controls of landslides in Rio de Janeiro: field evidence and modeling, *Catena*, *55*(2), 163-181.

Firomsa, M. and Abay, A., 2019. Landslide assessment and susceptibility zonation in Ebantu district of Oromia region, western Ethiopia, *Bulletin of Engineering Geology and the Environment*, *78*, 4229-4239.

Froude, M. J. and Petley, D. N., 2018. Global fatal landslide occurrence from 2004 to 2016, Nat. Hazards Earth Syst. Sci., 18, 2161–2181, https://doi.org/10.5194/nhess-18-2161-2018.

Gansser, A., 1964. Geology of the Himalayas. Wiley Inter Science, New York, 289

Gerrard, J, 1994. The landslide hazard in the Himalayas: geological control and human action. In *Geomorphology and natural hazards* (pp. 221-230).

Ghosh, T., Bhowmik, S., Jaiswal, P., Ghosh, S. and Kumar, D.,2020. Generating substantially complete landslide inventory using multiple data sources: a case study in Northwest Himalayas, India, *Journal of the Geological Society of India*, *95*(1), 45-58.

Giuseppe, F., Simoni, S., Godt, J. W., Lu, N. and Rigon, R., 2016. Geomorphological control on variably saturated hillslope hydrology and slope instability, *Water Resources Research*, *52*(6), 4590-4607.

Gupta, V., Kumar, S., Kaur, R. and Tandon, R. S., 2022. Regional-scale landslide susceptibility assessment for the hilly state of Uttarakhand, NW Himalaya, India. *Journal of Earth System Science*, *131*(1), 2.

Hasegawa, S., Dahal, R. K., Yamanaka, M., Bhandary, N. P., Yatabe, R. and Inagaki, H., 2009. Causes of large-scale landslides in the Lesser Himalaya of central Nepal, *Environmental geology*, *57*, 1423-1434.

Hennrich, K. and Crozier, M. J., 2004. A hillslope hydrology approach for catchment-scale slope stability analysis, *Earth Surface Processes and Landforms: The Journal of the British Geomorphological Research Group*, *29*(5), 599-610.

Huang, R., 2015. Understanding the mechanism of large-scale landslides, In *Engineering Geology for Society and Territory-Volume 2: Landslide Processes* (pp. 13-32). Springer International Publishing.

Hung, C., Liu, C. H. and Chang, C. M., 2018. Numerical Investigation of Rainfall-Induced Landslide in Mudstone Using Coupled Finite and Discrete Element Analysis, *Geofluids*, *2018*(1), 9192019.

Karimi-Sangchini, E., Emami, S. N., Shariat-Jafari, M., Rezazadeh, F. and Raeisi, H., 2020. Landslide hazard zonation using multivariate statistical models in the Doab Samsami watershed, Chaharmahal Va Bakhtiari Province, Iran, *Jordan J Earth Environ Sci*, *11*, 174-182.

Knapen, A., Kitutu, M. G., Poesen, J., Breugelmans, W., Deckers, J. and Muwanga, A., 2006. Landslides in a densely populated county at the footslopes of Mount Elgon (Uganda): characteristics and causal factors, *Geomorphology*, *73*(1-2), 149-165.

Lee, J. U., Cho, Y. C., Kim, M., Jang, S. J., Lee, J. and Kim, S., 2022. The effects of different geological conditions on landslide-triggering rainfall conditions in South Korea. *Water*, *14*(13), 2051.

Manchado, A. M. T., Ballesteros-Cánovas, J. A., Allen, S. and Stoffel, M., 2022. Deforestation controls landslide susceptibility in Far-Western Nepal, *Catena*, *219*, 106627.

McAdoo, B. G., Quak, M., Gnyawali, K. R., Adhikari, B. R., Devkota, S., Rajbhandari, P. L. and Sudmeier-Rieux, K., 2018. Roads and landslides in Nepal: how development affects environmental risk, *Natural Hazards and Earth System Sciences*, *18*(12), 3203-3210.

Mezughi, T. H., Akhir, J. M., Rafek, A. G. and Abdullah, I., 2011. Landslide susceptibility

assessment using frequency ratio model applied to an area along the EW highway (Gerik-Jeli), *American Journal of Environmental Sciences*, *7*(1), 43.

Moore, I. D., Gessler, P. E., Nielsen, G. A. E. and Peterson, G. A., 1993. Soil attribute prediction using terrain analysis, *Soil science society of america journal*, *57*(2), 443-452.

Mugagga, F., Kakembo, V. and Buyinza, M., 2012. A characterization of the physical properties of soil and the implications for landslide occurrence on the slopes of Mount Elgon, Eastern Uganda. *Natural hazards*, *60*, 1113-1131.

Muñoz-Torrero Manchado, A., Allen, S., Ballesteros-Cánovas, J.A., Dhakal, A., Dhital, M. R. and Stoffel, M., 2021. Three decades of landslide activity in western Nepal: new insights into trends and climate drivers. *Landslides* 18, 2001–2015 (2021). https://doi.org/10.1007/s10346-021-01632-6

Nakileza, B. R., Mugagga, F., Musali, P. and Nedala, S., 2022. Assessment of Landslide susceptibility and risk to road network in Mt Elgon, Uganda.

Nseka, D., Kakembo, V., Bamutaze, Y. and Mugagga, F., 2019. Analysis of topographic parameters underpinning landslide occurrence in Kigezi highlands of southwestern Uganda, *Natural Hazards*, *99*, 973-989.

Nugraha, H., Wacano, D., Dipayana, G. A., Cahyadi, A., Mutaqin, B. W. and Larasati, A., 2015. Geomorphometric characteristics of landslides in the Tinalah watershed, Menoreh Mountains, Yogyakarta, Indonesia, *Procedia Environmental Sciences*, *28*, 578-586.

Pardeshi, S. D., Autade, S. E. and Pardeshi, S. S., 2013. Landslide hazard assessment: recent trends and techniques, *SpringerPlus*, *2*, 1-11.

Paudyal, K. R., Maharjan, R. and Shrestha, B., 2024. Landslide susceiptibility mapping of the main boundary thrust region in Thungsingdanda-Bandipur section of Nawalparasi and Palpa Districts, Gandaki and Lumbini Provinces, Nepal, The Geographical Journal of Nepal. Vol. 17:23-52, 2024. DOI: https://doi.org/10.3126/gjn.v17i01.63934.

Paudyal, K.R. and Maharjan, R., 2023. Landslide susceptibility mapping of the Main Boundary Thrust region in Mandre-Khursanibari section of Arghakhanchi and Palpa districts, Lumbini province of Nepal, Nepalese Journal of Environmental Science, 11(2),35-53; https://doi.org/10.3126/njes.v11i2.58152

Paudyal, K. R., Devkota, K.C., Parajuli, B.P., Shakya, P. and Baskota, P., 2021. Landslide Susceptibility Assessment using open-source data in the far western Nepal Himalaya: A case study from selected local level units, *Journal of Institute of Science and Technology,* 26(2), 31-42 (2021) *ISSN: 2467-9062 (print),e-ISSN:2467-9240*. https://doi.org/10.3126/jist.v26i2.41327.

Paudyal K. R. and Maharjan R., 2022. Landslide susceptibility mapping of the Main Boundary Thrust (MBT) region in Tinau-Mathagadhi Section of Palpa District, Lumbini Province, Journal of Nepal Geological Society, vol. 63, pp. 99–108. *https://doi.org/10.3126/jngs.v63i01.50845*

Pokhrel, K. and Bhandari, B. P., 2019. Identification of Potential Landslide Susceptible Area in the Lesser Himalayan Terrain of Nepal, Journal of Geoscience and Environment Protection, 7, 24-38. https://doi.org/10.4236/gep.2019.711003

Pradhan, A. M. S., Dawadi, A. and Kim, Y. T.,2012. Use of different bivariate statistical landslide susceptibility methods: a case study of Khulekhani watershed, Nepal, *Journal of Nepal Geological Society*, *44*, 1-12.

Regmi, A.D., Yoshida, K., Pourghasemi, H.R., DhitaL, M. R. and Pradhan, B., 2014. Landslide susceptibility mapping along

Bhalubang — Shiwapur area of mid-Western Nepal using frequency ratio and conditional probability models, *J. Mt. Sci.* 11, 1266–1285 (2014). https://doi.org/10.1007/s11629-013-2847-6

Reichenbach, P., Rossi, M., Malamud, B. D., Mihir, M. and Guzzetti, F., 2018. A review of statistically-based landslide susceptibility models, *Earth-science reviews*, *180*, 60-91.

Sharma, K. K., Bhandary, N. P., Subedi, M. and Rajan, K. C., 2025. Integration of Landslide Susceptibility and Road Infrastructure Vulnerability for Risk Assessment and Mountain Road Resilience Enhancement, *Indian Geotechnical Journal*, 1-17.

Sharma, S. and Mahajan, A. K., 2019. A comparative assessment of information value, frequency ratio and analytical hierarchy process models for landslide susceptibility mapping of a Himalayan watershed, India, *Bulletin of Engineering Geology and the Environment*, *78*, 2431-2448.

Silalahi, F. E. S., Pamela, Arifianti, Y. and Hidayat, F., 2019. Landslide susceptibility assessment using frequency ratio model in Bogor, West Java, Indonesia, *Geoscience Letters*, *6*(1), 10.

Singh, A., Pal, S. and Kanungo, D. P., 2021. An integrated approach for landslide susceptibility–vulnerability–risk assessment of building infrastructures in hilly regions of India, *Environment, Development and Sustainability*, *23*(4), 5058-5095.

Sudmeier-Rieux, K., McAdoo, B., Devkota, S., Rajbhandari, P. C. L., Howell, J. and Sharma, S., 2019. Invited perspectives: mountain roads in Nepal at a new crossroads, Nat Hazards Earth Syst Sci 19:655–660

Talebi, A., Uijlenhoet, R. and Troch, P. A., 2008. Application of a probabilistic model of rainfall-induced shallow landslides to complex hollows, *Natural Hazards and Earth System Sciences*, *8*(4), 733-744.

Tarolli, P., Sofia, G. and Dalla Fontana, G., 2012. Geomorphic features extraction from high-resolution topography: landslide crowns and bank erosion, *Natural Hazards*, *61*, 65-83.

Thapa, D. and Bhandari, B., 2019. GIS-Based Frequency Ratio Method for Identification of Potential Landslide Susceptible Area in the Siwalik Zone of Chatara-Barahakshetra Section, Nepal, *Open Journal of Geology*, 9, 873-896. doi: 10.4236/ojg.2019.912096.

Thapa, D. and Bhandari, B. P., 2019. GIS-Based frequency ratio method for identification of potential landslide susceptible area in the Siwalik zone of Chatara-Barahakshetra section, Nepal, *Open Journal of Geology*, *9*(12), 873.

Thapa, P. B., Phuyal, B. and Shrestha, K. K., 2023. Spatial variability of slope movements in central and western Nepal Himalaya: Evaluating large-scale landslides to cut-slopes, *Journal of Nepal Geological Society*, *65*, 183-194.

Timalsina, A. and Bhandari, B. P., 2024. Hydrological influences of the landslide mechanisms: insight into the Aakhu Khola Watershed, Dhading District, Nepal, *Journal of Nepal Hydrogeological Association*, *1*, 67-78.

Tsou, C. Y., Chigira, M., Higaki, D., Sato, G., Yagi, H., Sato, H. P., Wakai, A., Dangol, V., Amatya, S.C. and Yatagai, A., 2018. Topographic and geologic controls on landslides induced by the 2015 Gorkha earthquake and its aftershocks: an example from the Trishuli Valley, central Nepal, *Landslides*, *15*, 953-965.

UNFCO, 2012. An overview of the Far Western Region of Nepal. United Nations Field Coordination Office (UNFCO) Dadeldhura, Nepal, Transition Support Strategy, RCHC Office, Nepal Worldpop (2020) WorldPop: population counts. In: Worldpop.org. https://www.worldpop.org/project/categories?id=3. Accessed 23 Sep 2020.

Van Westen, C. J., 1997. Statistical landslide hazard analysis. *Ilwis*, *2*, 73-84.

Zhang, J. Q., Liu, R. K., Deng, W., Khanal, N. R., Gurung, D. R., Murthy, M. S. R.and Wahid, S., 2016. Characteristics of landslide in Koshi River basin, central Himalaya, *Journal of Mountain Science*, *13*, 1711-1722.

Zhuang, J., Peng, J., Iqbal, J., Liu, T., Liu. N., Li, Y. and MA, P., 2015. Identification of landslide spatial distribution and susceptibility assessment in relation to topography in the Xi'an Region, Shaanxi Province, China, Front Earth Sci 9(3):449–462. https://doi.org/10.1007/S11707-014-0474-3

.